Metrol. Meas. Syst., Vol. 28 (2021) No. 3, pp. 413–438
DOI: 10.24425/mms.2021.137133

PAN POLSKA AKADEMIA NAUK

METROLOGY AND MEASUREMENT SYSTEMS
Index 330930, ISSN 0860-8229
www.metrology.wat.edu.pl

M&MS

A COMPARISON BETWEEN PROFILE AND AREAL SURFACE ROUGHNESS PARAMETERS

Baofeng He, Siyuan Ding, Zhaoyao Shi

Beijing University of Technology, Faculty of Materials and Manufacturing, Beijing Engineering Research Center of Precision Measurement Technology and Instruments, 100 Ping Le Yuan, Chaoyang District, Beijing 100124, China
(✉ *baofenghe@aliyun.com*, +86 18610040321, *dsy9961@163.com*, *shizhaoyao@bjut.com*)

Abstract

Surface roughness has an important influence on the service performance and life of parts. Areal surface roughness has the advantage of accurately and comprehensively characterizing surface microtopography. Understanding the relationship and distinction between profile and areal surface roughness is conducive to deepening the study of areal surface roughness and improving its application. In this paper, the concepts, development, and applications of surface roughness in the profile and the areal are summarized from the aspect of evaluation parameters. The relationships and differences between surface roughness in the profile and the areal are analyzed for each aspect, and future development trends are identified.

Keywords: profile surface roughness, areal surface roughness, filtration techniques, evaluation parameters.

1. Introduction

A machined surface is composed of a series of peaks and valleys with different heights and spacings. Surface roughness refers to microscopic geometric features of tiny peaks and valleys on a machined surface, usually arranged in a non-deterministic way or at least with stochastic feature components. This microscopic property has an important influence on the sealing, wear resistance, fatigue strength, contact stiffness, and corrosion resistance of the surface of a part and the factors related with its performance and life [1]. Surface roughness is classified as either profile or areal. The surface profile is obtained by intersecting the real surface with a specified plane. Quantitative evaluation of profile surface roughness is performed on the profile of the surface to be measured, and the evaluation of areal roughness is performed on the sampling area.

Early studies of surface roughness were qualitative. For example, in the 1930s, German manufacturers used triangular symbols combined with visual methods to specify the roughness of a machined surface. At the same time, Abbott in the United States and Schmaltz in Germany

Article history: received February 3, 2021; revised May 18, 2021; accepted May 19, 2021; available online May 27, 2021.

launched research on surface roughness parameters and instruments [2, 3]. Since the 1940s, a number of countries have developed standards for assessment of surface roughness which are based on the mean line system. After the development of international standards, the revised standards of various countries have moved closer to international standards and are basically consistent. The analysis of surface roughness has been developed for more than 100 years, and the profile roughness analysis method has been widely used in manufacturing processes [4]. However, profile roughness has drawbacks; for example, a profile can poorly express surface topography with a specific non-isotropic structure and care has to be taken of the orientation of the profile with respect to lay. The limitations of profile roughness have encouraged the development of areal roughness. The analysis of areal surface topography first appeared in 1967, and Williamson established the first micro-surface topography measurement system at that time [5]. In the 1970s, Nayak, Sayles, and Thomas first defined peaks and valleys on measured areal surface data on axes [6, 7]. In the late 1980s, the advent of personal computers made it possible to analyze areal roughness [8]. Research on areal characterization experienced its first important turning point in April 1990 with an areal roughness research project led by the University of Birmingham which was strongly supported by the European Community. In this project, Stout et al. made outstanding contributions [9]. The "Blue Book" published as a result of the project presents a basic set of standards for areal roughness assessment [10]. In May 1998, the European Union gave funds to the University of Huddersfield for the SURFSTAND project which evaluated and improved the Birmingham 14 parameters, developed robust and wavelet filtration techniques, and studied the calibration of areal roughness instruments [11]. After the completion of large projects such as SURFSTAND and AUTOSURF (a project to solve surface texture problems of the automotive industry), the *International Standardization Organization* (ISO) began to develop areal roughness standards. In January 2003, ISO/TC 213 established the working groups WG 16 to develop international standards on roughness parameters and measurement instrumentation in particular with view to areal roughness and WG 15 to develop the standards on filtration [12]. In May 2003, the "Green Book" containing all of the results of the SURFSTAND project was published [13]. At the end of 2005 ISO assigned the number ISO 25178 to the areal surface topography standard, and the surface metrology changed from profile to areal [14].

It can be seen that areal roughness is developed from the profile. However, the characterization of areal roughness does not simply extend from the profile to the areal. In addition to extending the profile part, areal roughness presents a new concept. Profile and areal roughness are correlated to each other yet differences exist. Understanding the comparison between profile and areal roughness can be of great help in understanding the topography and function of a surface being measured. This paper will introduce the connections and distinctions between profile and areal surface roughness parameters.

2. Filtering technique

The machined surface of a part is usually composed of surface components of different spatial frequencies. Filtering out long-wave components in the measured surface data is a prerequisite for assessing the microscopic surface topography by surface roughness parameters. International standards divide filters into profile and areal ones. Gaussian filters are recommended in the current international standards for surface roughness assessment because of their linear phase and ease of calculation.

2.1. Profile filtering

The profile filter can divide the profile into long- and short-wave components. The 2D surface topography based on the lateral scale can be divided into three components: roughness, waviness and primary profile. Components are divided by λ_s, λ_c, and λ_f profile filters. λ_s is the filter that defines the intersection between the roughness and the even shorter wave components present in a surface. λ_c is the filter that defines the intersection between the roughness and waviness components. λ_f is the filter that defines the intersection between the waviness and the even longer wave components. Different types of filters can be used to select the cut-off wavelength of long or short waves. Long-wave filtering eliminates the effect of waviness on the roughness measurement in the actual surface profile, and short-wave filtering removes components that are shorter than the roughness wavelength.

The ISO 16610 series introduces both linear and robust types of Gaussian filters [15, 16]. A conventional profile Gaussian filter uses a convolution integral method to obtain a mean line. However, since the Gaussian filter has end effects, the Gaussian filter mean line usually does not define the end profile. The profile Gaussian regression filter uses least squares to fit the surface profile. The mean line defines the function value of each point on the measured surface profile, which can solve the end effects of the Gaussian filter. The robust profile Gaussian filter solves the problem that the mean line is distorted by outliers (high peaks or deep valleys on the surface being measured). The robust profile Gaussian regression filter can simultaneously exhibit the excellent characteristics of the above two filters.

2.2. Areal filtering

The concept of areal filtering is derived from profile filtering. Areal filters can divide the measured areal surface topography data into components of different scales. ISO 25178-2 divides areal filters into three types: S-filter, L-filter, and F-operation. The S-filter can remove unwanted small-scale components, such as measurement noise in the measured data, to obtain the primary surface. The L-filter can remove unneeded large-scale components in the measurement data. F-operation refers to the removal of the nominal form on the primary surface to avoid the surface shape of the sample being measured from shifting the measured micromorphology. The S–F surface is obtained by performing an F-operation on the primary surface, as shown in Fig. 1; the S–L surface is obtained by removing the large-scale component using an L-filter on the S–F

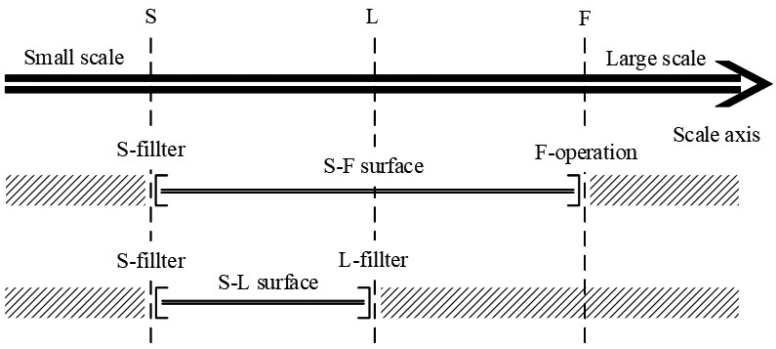

Fig. 1. Relationship between scale-limited surface and surface filter.

surface. The scale-limited surface refers to an S–F surface or S–L surface whose definition area can be used to characterize areal roughness parameters.

Robust profile Gaussian filters have the advantage of being insensitive to outliers, and the regression filtering technique including robust algorithms is also applicable to areal surface filtering. The robust areal Gaussian regression filter is nonlinear, and is based on the areal Gaussian weighting function, the dual weight function, and the complete polynomial modeling of the surface. The weighting function of the filter depends on the coordinate values of the relative reference surface and the position of the weighting function on the surface. Since the robust algorithm is derived from statistics, the robust areal Gaussian regression filter has a wider range of application. The characteristics of the three areal Gaussian filters are shown in Table 1.

Table 1. Characteristics of three areal Gaussian filters.

Filters	Characteristic	Applicable surface
Areal Gaussian filter	Recommended for international standards	Smooth, no high peaks or deep valleys, non-small size
Areal Gaussian regression filter	The end effects are solved; the scale separation is more accurate	Smooth, no high peaks or deep valleys
Robust areal Gaussian regression filter	Reduce the impact of outliers	Honed, structured surface processed by laser, metal matrix composite

2.3. Comparison between profile filtering and areal filtering

The areal filtering technique is developed from the profile filtering technique, and the types of areal filters correspond to those of profile filters. The flow of parameters obtained by a profile filter and by surface filters acting on surface topography at different scales is shown in Fig. 2. In the 2D and areal roughness filtering process, the areal S–F surface corresponds to a 2D primary profile, the S-filter corresponds to a λ_s profile filter, and the F-operation corresponds to removal of the nominal form. The areal S–L surface corresponds to a roughness profile defined by a 2D surface topography, while the S-filter corresponds to a λ_s profile filter, and the L-filter corresponds to a λ_c profile filter. In an areal S–F surface, when the S-filter corresponds to a λ_c profile filter and the effect of the F-operation corresponds to the removal of the nominal form, and the areal surface corresponds to the waviness profile of the 2D surface.

The areal filtering technique has its own unique filtering method which is defined in both spatial and frequency domains. The biggest difference between areal and 2D roughness evaluation is the use of filters [17]. For example, the 2D profile extracted from the measured areal topography is different from that measured according to the 2D roughness standard because they use different algorithms. In addition, when 2D roughness is measured using a stylus instrument, the roughness profile is mainly extracted by the profile filters, and the scanning path of the instrument is usually perpendicular to the surface texture. However, the filtering process of areal filters is performed simultaneously in the x- and y- directions, and the two directions are not necessarily perpendicular to the surface texture. Therefore, even if the same parameters and the same type of profile and areal filters are set on the same measured surface, the results are not necessarily the same. Similar to profile filtering, before areal filtering, it is necessary to select appropriate types of filters and nesting indices according to the type of surface to be measured to obtain the best filtering effect.

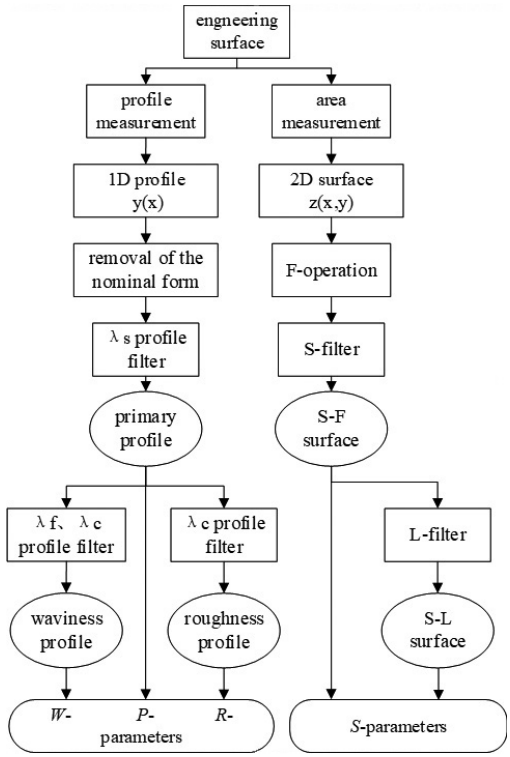

Fig. 2. Flowchart for profile filtering and areal filtering.

3. Characterization of surface roughness

3.1. Roughness evaluation parameters

Roughness evaluation parameters contain information such as amplitude and spacing of the surface topography to be measured. The profile roughness parameter is based on the profile of the surface to be measured, and the areal parameter is based on the measured area. Areal roughness parameters are derived from profile roughness parameters, and they have similarities and differences.

3.1.1. Profile roughness parameters and applications

Profile roughness parameters are usually calculated on the profile which is perpendicular to the most prominent surface texture direction, and have the four main types of amplitude, spacing, hybrid, and curves and related parameters. Calculation of the parameters depends on the sampling or evaluation length. Sampling length is the length in the direction of the x axis used for identifying the irregularities that characterise the profile under evaluation. Evaluation length is the total length in the x axis used for the assessment of the profile under evaluation. It is normal practice to evaluate roughness and waviness profiles over several successive sampling lengths, the sum of which gives the evaluation length. Profile roughness evaluation parameters are widely used in manufacturing processes. Table 2 summarizes the profile roughness parameters and their applications [18–20].

Table 2. Summary of profile roughness parameters.

Class of parameters	Definition		Symbol	Determined within		Description and application	
				Sampling length	Evaluation length		
Amplitude parameters	Peak and valley	Maximum profile peak height	Rp	√		Measured parameter values may be affected by dust and selection of measurement areas	Friction and wear [21]
		Maximum profile valley depth	Rv	√		Measured parameter values may be affected by dirt, scratches and measurement areas	Corrosion resistance [22]; detecting cracks on surface [23]
		Maximum height of profile	Rz	√		Measured parameter values may be affected by dust, dirt, scratches, and measurement areas; $Rt \geq Rz$	Mating part surface under high stress or alternating stress [24]; detecting outliers; safety analysis of oil lubrication film of sliding bearing [25]; analysis of electrical contact effectiveness [26]
		Total height of profile	Rt		√		
		Mean height of profile elements	Rc	√		Calculation of parameter values must determine height and spacing of profile elements	Analysis of adhesion [27]
	Average of ordinates	Arithmetical mean deviation of the assessed profile	Ra	√		One of the most commonly used and most readily available roughness parameters, characterizing precision machined surfaces is not sensitive; Ra values may be the same for surfaces with different spatial periodicity	Manufacturing control
		Root mean square deviation of the assessed profile	Rq	√		Good statistical significance	Optical or electronic components [28]; detecting defects in precision-machined surfaces [29]
		Skewness of the assessed profile	Rsk	√		Parameters are greatly affected by outliers; acquisition of parameters requires use of specific filters; poor repeatability	Plateau honing process with parameter Rku [30]; lubricant retention; cleaning [31]; surface wettability [32]
		Kurtosis of the assessed profile	Rku	√		Parameters are greatly affected by outliers; poor repeatability	Tools-condition monitoring [33]; monitoring the surface wear of a part with parameter Rsk

Table 2 [cont.]

Class of parameters	Definition		Symbol	Determined within		Description and application	
				Sampling length	Evaluation length		
Spacing parameters	Mean width of the profile elements		Rsm	√		It is difficult to distinguish the surface of a smooth waveform; these parameters should usually be used in conjunction with other parameters	Tool-condition monitoring [34]; deciding on correct filter, coating [35]; friction; sealing [36]; punch forming [37]; fluid flow [38]
Hybrid parameters	Root mean square slope of the assessed profile		$R\Delta q$	√		Parameter values are sensitive to outliers	Extremely smooth surface, friction [39]; reflectivity; elasticity; wear [40]; noise [41]; adhesion [57]
Curves and related parameters	ISO 4287: 1997	Material ratio of the profile	$Rmr(c)$		√	This series of parameters can reflect the running-in characteristics and life of the mating surface, substrate properties of the surface, and deep valley lubrication characteristics; material ratio curve of the profile and profile height amplitude curve can be transformed by differentiation and integration	Simulate and predict wear process; bearing surface; inner surface of a cylinder bore in the automotive industry; wear; contact stiffness [42]
		Material ratio curve of the profile	Material ratio curve		√		
		Profile section height difference	$R\Delta c$		√		
		Relative material ratio	Rmr		√		
		Profile height amplitude curve	profile height amplitude curve		√		
	ISO 13565-2: 1996	Core roughness depth	Rk		√	This series of parameters can only be used with an S-shaped material ratio curve of the profile; parameter value is affected by the shape of the tool; can be used for functional evaluation of high-stress surfaces such as those with stratified functional properties; honing, grinding and polishing; parameters correspond to surface friction, wear, and lubrication properties [43]; Rk can be used to estimate the cylinder life of a car [44]; M_{r1} and M_{r2} can be used to control product quality [45]; Rpk can be used for run-in analysis of the surface of a part; Rvk can be used to analyze surface lubricant retention of a part, but presence of pores may cause a misleading parameter value [46]	
		Material portion	M_{r1}, M_{r2}		√		
		Reduced peak height	Rpk		√		
		Reduced valley depths	Rvk		√		

Metrol. Meas. Syst., Vol. 28 (2021), No. 3, pp. 413–438
DOI: 10.24425/mms.2021.137133

3.1.2. Areal parameters and applications

Early areal parameters were mostly derived from profile parameters, and there was no uniform areal parameter standard at that time. Therefore, areal roughness measuring instruments produced by different manufacturers could produce different results. In the 1980s, Whitehouse and Phillips defined three areal parameters in detail [47, 48]. In the 1990s, Stout *et al*. systematically studied the areal parameters defined by the famous Birmingham 14 parameters. However, the actual application of these 14 parameters was not confirmed [49]. In 1996, the ISO established a new Technical Committee, TC 213; one of its main objectives is to carry out basic research work on areal parameters. In 2005, ISO/TC 213 divided areal parameters into the five categories of spatial, height, hybrid, functional, and volume parameters. Part 2 of the ISO 25178 International Standard, which contains terms and definitions for areal surface texture parameters, was published in 2012.

Areal parameters are calculated on a scale-limited surface and consist mainly of field and feature parameters. Field parameters are based on statistical principles and express information, such as mean values, deviations, extreme values, and specific features of a scale-limited surface. Field parameters consist mainly of *S*- and *V*-parameters. *S*-parameters mainly contain information such as the height and spatial frequency of the surface to be measured. *V*-parameters provide basic volume information of an areal surface based on the material ratio curve.

Table 3 summarizes field parameters and related applications [13, 50, 51]. A lot of researches have stressed the significance of field parameters in quantifying surface features or textures. For height parameters, the value of S_z of uncoated titanium plasma sprayed implant surfaces was significantly higher than that of the TiN-coated titanium plasma sprayed surfaces [52]. S_{Sk} is

Table 3. Summary of field parameters.

Class of parameter	Definition	Symbol	Description	Application
Height parameters	Arithmetical mean height	S_a	When characterizing different machined surfaces, parameter values may not change much, parameter values may be the same for different surfaces; S_q is more statistically significant than S_a	Engineering surface
	Root mean square height of the scale-limited surface	S_q		Related to the scattering of light on the surface; [4] be used on surface of optical components; [60] surface of dental implant bonding cement; [61] bacterial adhesion of composite resins; [62] cell viability on anodic porous alumina substrates; [63] adhesion of dental restorative composite; [64]
	Maximum peak height	S_p	Extreme type parameter is greatly affected by peak, dale, or pit of anomaly, so must be measured multiple times, and filter parameters adjusted to obtain more accurate values; S_p is positive and S_v is negative	Sliding mating surface [65]
	Maximum pit depth	S_v		Lubrication, coating [66]
	Maximum height of scale limited surface	S_z		S-F surface filtered with larger nesting index S-filter; detecting surface anomalies (burrs); sealing; coating
	Skewness of the scale-limited surface	S_{sk}	Greatly affected by peak, dale, or pit of anomaly, so must be measured multiple times, and filter parameters adjusted to obtain more accurate values; parameter is related to symmetry of surface, cannot distinguish between height peak and deep dale or pit features, but can prove their existence	Bearing surface; honing processing; bearing capacity analysis of surface of part; porosity; wear; [67] surface of nanocomposite thin films; [68] surface of glass-ceramic porous orbital implants [69]

Table 3 [cont.]

Class of parameter		Definition	Symbol	Description	Application
Height parameters		Kurtosis of the scale-limited surface	S_{ku}	This parameter is greatly affected by the peak, dale, or pit of the anomaly, so it is necessary to measure multiple times and adjust the filter parameters to obtain more accurate values; poor stability	Honing processing; defect detection on the surface of parts; surface of nanocomposite thin films; [68] surface of glass-ceramic porous orbital implants [69]
Spatial parameters		Auto-correlation length	S_{al}	For anisotropic surfaces, parameter value is larger if surface is dominated by low-frequency components, and smaller with high frequency	Analysis of interaction of mating surfaces, friction and wear; [70] surface texture detection; [71] electromagnetic properties of surface of part [72]
		Texture aspect ratio	S_{tr}	Parameter values are related to intensity of surface texture (uniformity of surface texture), and the parameter value ranges from 0 to 1. When S_{tr} is close to 1, the measured surface is isotropic, otherwise, it is anisotropic	Surface of stratified functional properties; [73] monitoring of vibration of machine tool [74]
Hybrid parameters		Root mean square gradient of the scale-limited surface	S_{dq}	Parameters are affected by amplitude and spacing of surface texture; for surfaces with the same S_a value, the wider the surface spacing the smaller the value of Sdq	Sealing; light reflex; [75] wear; electromagnetic contact; wettability; [76] appearance quality
		Developed interfacial area ratio of the scale-limited surface	S_{dr}	The parameter is greatly affected by the number of sampling points in the x- and y-directions, along with the sampling interval	Complexity of surface; adhesion; [56] coating; osteopathic medicine; [77] surfaces of implants before and after insertion [78]
Miscellaneous parameters		Texture direction of the scale-limited surface	S_{td}	Contains direction information of surface texture; represent the uniformity of the surface texture together with S_{tr} [79]	Reference positioning; [80] surface texture detection; sealing; [81] monitoring of rough machining process [82]
Functions and related parameters		Areal material ratio of the scale-limited surface	$S_{mr(c)}$	Height c can be calculated according to best fit least squares reference plane or areal material ratio function of scale-limited surface	Inner surface of cylinder bore in automotive industry; analysis of bearing load-carrying capacity
		Inverse areal material ratio of the scale-limited surface	$S_{mc(mr)}$		Sealing design [83]
		Peak extreme height	S_{xp}	Does not take into account a small fraction of the highest peak, represents height of area where surface friction property plays a major role	Analysis of surface bearing and wear resistance of parts

Table 3 [cont.]

Class of parameter		Definition	Symbol	Description	Application	
Functions and related parameters	Areal parameters for scale-limited stratified functional surfaces	Core height	S_k	Material ratio curve based on parameters is built on a areal surface; robust areal Gaussian filter is typically used before calculation to mitigate effects of outliers, before calculating the series of parameters, the surface is decomposed into peak, core, and valley zones, and the amplitude or volume is calculated based on the three parts	Automobile industry; for surfaces with height peak and deep dale or pit characteristics; [84] can be used instead of parameters such as S_z; lower S_k allows better sliding contact between the contact surfaces; surfaces of functional protective coatings [85]	
		Reduced peak height	S_{pk}		Analysis of surface contact stress, higher S_{pk} values indicate higher contact stress	
		Reduced dale height	S_{pk}		Lubricant retention; debris entrapment; the S_{pk}/S_k, S_{vk}/S_k, S_{pk}/S_{vk} can be used to measure load carrying capacity or contact stress of machined surfaces	
		Material ratio	S_{mr11}, S_{mr11}		Running-in analysis of surface of part, lubricant retention	
	Void volume	Dale void volume of the scale-limited surface	V_{vv}	Characterises the volume of fluid retention in the deepest valleys of the surface, and less affected by the wear process	Can be used to describe surface shape and distinguish surface volume characteristics with different roughness levels [86]	Analysis of surface wear, running-in, and bearing; sealing; lubricant retention
		Void core volume of the scale-limited surface	V_{vc}	Represents core space available for surface of part after run-in period		
	Material volume	Peak material volume of the scale-limited surface	V_{mp}	Similar to S_{pk}, can be used to analyze worn part of mating surface, determined wear behaviour by comparison of the V_{mp} before and after the abrasion		Analysis of fluid motion on surface of part; [87] lubricant retention; debris entrapment; coating; texture evaluation of mating surface [88]
		Core material volume of the scale-limited surface	V_{mc}	Indicates parts of surface that do not touch each other during part-fitting process; not related to lubrication		

a measurement of symmetry of surface deviations for the mean reference plane. For a surface with a symmetric height distribution, such as a Gaussian surface, $S_{Sk} = 0$. For an asymmetric distribution of topography heights, $S_{Sk} < 0$ if the distribution has a longer tail in the downward direction of the mean plane, or $S_{Sk} > 0$ if the distribution has a longer tail in the upward direction of the mean plane. The smaller friction coefficient of the measured surface is accompanied by a larger value of S_{ku} and a smaller value of S_{sk}. [53] S_q and S_a have a strong linear correlation with surface glossiness, and the smaller the parameter value, the higher the glossiness [54]. For

hybrid parameters, S_{dq} could distinguish the surfaces with similar values of S_a parameter, and S_{dr} and S_{dq} were able to distinguish the optical properties and coating performance between the turned and etched surfaces which cannot be distinguished by height or spatial parameters [55]. S_{dr} and S_{dq} showed a good correlation to friction (R^2 of 0.72 and 0.70) on the surface of the milled die steel sheet [56]. For the functions and related parameters, the higher value of $S_{mr©}$ indicates better bearing and wear properties [57]. The lubricant retention capacity increased with the higher value of V_{vc} or V_{vv} within a certain range [58]. The values of V_{mp} decrease after the abrasion [59].

3.1.3. Comparison between profile and areal roughness parameters

Surface roughness parameters are tolerance specifications and means of communication for engineering design and manufacturing. Profile parameters use one -dimensional filters, whereas areal roughness parameters use two = dimensional filters. Due to the difference of the algorithms of these two filters, profile and areal roughness parameters cannot be directly compared. However, this does not mean that they can completely differ from each other. They have similarities and differences.

Profile parameters are named based on the profile type (roughness, waviness, and original profile) used to calculate the parameters. For example, a profile roughness parameter has the prefix R. In areal surface topography analysis, the scales required for research in different directions can differ, $e.g.$ when applying surface topography in micro-elastohydrodynamic lubrication [89]. Areal parameters are classified as either S or V, according to the content information.

Profile roughness parameters are calculated according to sampling or evaluation length. Areal parameters still define the concept of evaluation and definition areas, but these have the same size by default. Calculating roughness requires reference to the measured height. The profile parameter refers to the reference line, and the areal parameter corresponds to the reference plane which is derived from profile roughness.

Areal height parameters can be used to describe the amplitude information on the surface of the part to be measured. This type of parameter is derived from the corresponding profile amplitude parameter. For example, there are also parameters from the Sq family: Spq, Svq and Smq which have 2D equivalents: Rpq, Rvq and Rmq. Since the extreme values measured in profile are usually not in the true extreme position on the areal surface, the height parameter values representing the extreme values of areal roughness such as S_z, are generally larger than the corresponding parameter values of the extreme value parameter R_z representing the amplitude of a profile [90]. The values of R_z and S_z were compared in characterizing the surface subjected to hard turning, belt grinding and superfinishing, and the results have showed that the values of R_z were all smaller than S_z for the three surfaces [91, 92].

Profile spacing parameters describe the degree of density of peaks and valleys on the surface profile. Areal spatial parameters are based on the areal *autocorrelation function* (*ACF*), and they describe the spatial characteristics of the surface to be measured. In addition to information on the dominant frequency component of the surface to be measured, areal parameters can also be used to evaluate whether the surface is isotropic or anisotropic. The areal parameter S_{al} is defined as the shortest horizontal distance at which $ACF(t_x, t_y)$ decays to a specified value $s (0 \leq s \leq 1)$. S_{tr} is defined as the ratio of the shortest to the longest horizontal distance of $ACF(t_x, t_y)$ decaying to the specified value s. S_{tr} has no equivalent parameter in the profile parameters. Surface information on an isotropic surface can be acquired using profile roughness measurement methods and characterized by profile roughness parameters. When measuring an anisotropic surface using profile measurement methods, it is necessary to consider the direction

of the surface to be measured. For example, international standards recommend a measurement direction perpendicular to surface texture. However, areal roughness measurement and parameter characterization need not consider the isotropy or anisotropy of the surface [93].

The profile hybrid parameter $R\Delta q$ is the root mean square value of the ordinate slope dZ/dX within the sampling length. Areal hybrid parameters contain both the amplitude and spatial information on the surface. S_{dq} and S_{dr} characterize the slope and developed interfacial area, respectively, of the areal surface topography. S_{dq} is derived from the profile parameter relative length of the profile (l_0), and S_{dr} is only applicable to areal surface topography analysis [94]. The effect of surface topography on shear strength of lap adhesive joints was analyzed. Compared with the height and spatial parameters, the areal hybrid parameters have stronger correlation with the shear strength. The values of linear correlation coefficients R of the parameters S_{dq}, S_{dr} and shear strength are 0.74 and 0.75 respectively, and the profile hybrid parameter $R\Delta q$ and shear strength is 0.72.

S_{td} is a miscellaneous areal parameter. The angular spectrum $f_{\mathrm{APS}}(s)$ is the power spectrum for a given direction s with respect to the specified direction θ in the plane of the definition area, and is expressed mathematically as:

$$f_{\mathrm{APS}}(s) = \int_{R_2}^{R_1} r\,|F\,[(r\sin(s-\theta), r\cos(s-\theta))]|^2\,\mathrm{d}r, \tag{1}$$

where R_1 and R_2 define the integral range in the radial direction. S_{td} is the angle of the absolute maximum value of the angle spectrum with respect to the specified direction θ. This parameter provides direction information for the areal surface texture, and has no corresponding profile parameter.

Similar to profile, the areal functions and related parameters are based on the material ratio curve. Material ratio curves can be developed by the same way in 2D and 3D analyses. The material ratio curve of the profile is calculated from the maximum peak of the profile and is therefore susceptible to outliers. However, the areal material ratio curve is calculated from the reference plane and therefore has a higher reliability. The profile and areal curves are drawn using robust Gaussian regression filters of different dimensions. The areal functions and related parameters describe the support, lubrication, friction and wear properties of the surface to be measured. $S_{mr}(c)$ is the ratio of the material area at a specified c to the evaluation area. This parameter can more accurately reflect the surface topography of the bearing area compared to the corresponding profile parameter $R_{mr}(c)$. It can also provide information on volume parameters. The scale-limited stratified functional surfaces refer to the surfaces with composite machining features, such as lapped or honed surfaces. The areal parameters for scale-limited stratified functional surfaces (S_k series parameters) are derived from the R_k series parameters. The equivalent straight line is calculated for the central region of the material ratio curve which includes 40% of the measured profile points. This type of parameter is mainly used to evaluate parts with high mechanical stress on the surface, and this type of evaluation is greatly affected by the resolution of the measuring instruments [95]. Unlike the R_k series parameters, the basic mathematical theory of the S_k series parameters is strengthened, and the determination of the equivalent straight line makes the application of this series of parameters more general. The areal volume parameters have evolved and improved since the Birmingham 14 parameters. Their meanings are more related to the application of surface functions, and the functional information provided is more stable. The volume parameters can describe the shape of a surface, and they can distinguish the volume characteristics of the surface of a part with different roughness levels, which has practical

significance [96]. For example, the parameter values of S_k series and the volume parameters were compared for the surfaces (ground, honed and EDM surface) with different roughness levels, and the results showed that the values of S_k and volume family varied significantly for different roughness levels [97]. The profile and areal roughness of the cylinder liner after plateau honing were analyzed in terms of parameter correlation. The parameters R_k and R_{pk} (linear correlation coefficient $R = 0.72$), and Mr_1 and Mr_2 ($R = 0.97$) have a high correlation among the R_k series parameters. Similar to the results of the R_k series parameters, S_k and S_{pk} ($R = 0.8$), S_{mr1} and S_{mr2} ($R = 0.85$) have a higher correlation as well. In the study of combining process parameters, allthe parameters R_k, R_{vk}, and M_{r2} maintained high correlations with coarse honing pressure P_v and plateau honing time t. However, in the S_k series parameters, S_{mr2} had a higher correlation with P_v and t, and S_k, S_{vk} only maintained a higher correlation with P_v. Therefore, the conclusions for application of areal parameters should be obtained by experiment rather than by analogy with profile parameters [47]. The scattering ranges for the surface roughness parameters were analyzed in the research of material of composite PBT+10% glass beads. It was found that the averages of the areal parameters S_a, S_q and S_{sk} were 5% to 15% larger than the values of the profile parameters R_a, R_q and R_{sk}, and the scattering interval was narrower [100]. Table 4 summarizes the relationship between profile and areal parameters.

Table 4. Relationship between profile and areal roughness parameters.

Profile		**Relationship**	**Areal**	
Amplitude parameters	Rp, Rv, Rz, Rc, Rt, Ra, Rq, Rsk, Rku	Since the manufacturing industry user wants coherence between the profile amplitude parameters and areal height parameters, the latter are derived from the former; the value of the extremum parameter in areal height parameters is usually greater than its profile equivalent	Height parameters	S_p, S_v, S_z, S_a, S_q, S_{sk}, S_{ku}
Spacing parameters	Rsm	Both profile and areal parameters contain information on frequency components of the surface to be measured, but the areal spatial parameters can determine isotropy or anisotropy of the surface of the part	Spatial parameters	S_{al}, S_{tr}
Hybrid parameters	$R\Delta q$	Areal parameter S_{dq} is derived from profile parameter $R\Delta q$; the areal parameter S_{dr} is only suitable for areal surface topography analysis	Hybrid parameters	S_{dq}, S_{dr}
		Provides direction information for areal surface texture	Miscellaneous parameters	S_{td}
Curves and related parameters	$Rmr(c)$, $R\Delta c$, Rmr, Rk, Rpk, Rvk, M_{r1}, M_{r2}	Areal functions and related parameters are derived from profile equivalents; the material ratio curve of the profile is susceptible to outliers; an areal material ratio curve calculated based on the reference plane is more reliable; theory of S_k series parameters is strengthened compared to Rk series parameters; volume parameters provide detailed material and core volume information for better numerical and functional evaluation of surface topography	Functions and related parameters	$S_{mr(c)}$, $S_{mc(mr)}$, S_{xp}, S_k, S_{pk}, S_{vk}, S_{mr1}, S_{mr2}, V_{vv}, V_{vc}, V_{mp}, V_{mc}

3.2. Feature characterization

The surface of a part usually has surface features of different scales. The type, size and composition of these features can greatly influence surface functions such as optical properties and coating. Therefore, it is necessary to describe the geometric features of the surface of the part. Feature characterization has two forms, profile and areal, and the characterization parameters are also divided into two dimensions. The feature parameters can characterize the features and relationships of the surface texture pattern being measured.

3.2.1. Profile motif method

The profile motif method was developed and applied in the French automotive industry in the 1970s to solve the functional problems of surface textures based on roughness and waviness parameters analysis [98].

The profile roughness motif is obtained by using the operation set with the limit value A instead of using filters, and the recommended value of A is given in the ISO 12085 standard. There are three roughness parameters in the profile motif method, namely, the mean spacing of roughness motifs AR, mean depth of roughness motifs R, and maximum depth of profile irregularity Rx. These parameters are calculated within the evaluation length and apply to the 16% rule. When calculating a series of parameters, it is usually necessary to first remove small local peaks and find all of the peaks and valleys that define individual roughness motifs which are combined, after which Rx is calculated. Finally, the depths of the peaks and valleys are corrected and$R$ and AR are calculated. Table 5 summarizes the roughness parameters of the profile motif method and their related applications [99].

Table 5. Summary of profile motif parameters.

Definition	Symbol	Application
Mean spacing of roughness motifs	AR	Electroplating
Mean depth of roughness motifs	R	Analysis of lubricated slipping, rolling, dry friction, fluid friction, dynamic sealing of mating surface; adherence; electrolytic coating; corrosion resistance; appearance
Maximum depth of profile irregularity	Rx	Dynamic and static sealing; corrosion resistance; analysis of fatigue strengths with stress

3.2.2. Areal feature characterization

It is often necessary to segment a surface before identifying the areal surface features. The feature parameters have been included in Part 2 of ISO 25178, and the segmentation technique is considered a class of filters included in ISO 16610 Part 85.

Areal feature characterization is mainly based on pattern-recognition techniques, and the segmentation method is used to extract the topographic features predefined by the scale-defined surface from the measured surface. The steps to determine the feature parameters are shown in Fig. 3.

The format of the convention of the feature parameters is as follows: FC, feature, pruning, purpose, attributes, statistics, where the feature characterization is indicated by FC. For example, the density of peaks S_{pd} can be expressed as: (FC; H; Wolf pruning: 5%; All; Count; Density).

Metrol. Meas. Syst., Vol. 28 (2021), No. 3, pp. 413–438
DOI: 10.24425/mms.2021.137133

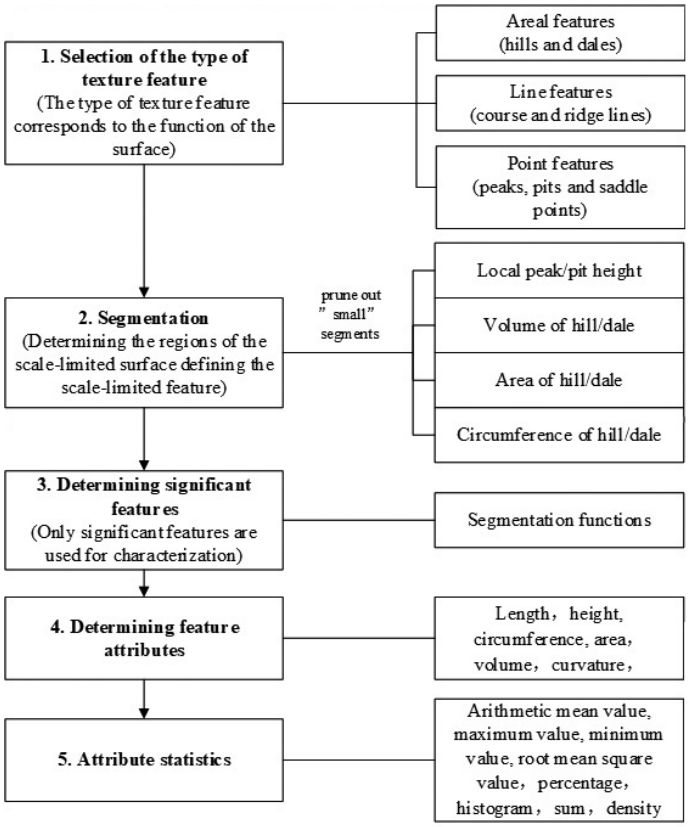

Fig. 3. Flowchart for areal feature characterization.

ISO 25178 Part 2 defines nine feature parameters. The density of peaks S_{pd} is usually used in conjunction with extreme height parameters such as S_{5p} or S_{5v}. Calculating the arithmetic mean peak curvature S_{pc} only takes into account significant peaks or dales. If the parameter value is larger, the peak on the surface is steeper, and if it is smaller, the peak is less steep. The parameter of ten-point height of surface S_{10z} is calculated as $S_{10z} = S_{5p} + S_{5v}$. The parameters of five-point peak height S_{5p} and five-point pit height S_{5v} are positive, and they only consider the peaks or pits of the five largest height values. The mean dale area $S_{da}(c)$ and mean hill area $S_{ha}(c)$ refer to the area projected to the horizontal plane. The parameters of the mean dale volume $S_{dv}(c)$, mean hill volume $S_{hv}(c)$, $S_{da}(c)$, and $S_{ha}(c)$ can be calculated according to whether they are open or closed at height c. Table 6 summarizes some of the applications of this series of parameters.

In addition to the applications in Table 6, S_{pd} can be used in the analysis of mating surfaces and abrasion, and S_{pc} can be used in the analysis of sliding friction and deformation of static contact. Areal feature parameters have been continuously extended to applications such as thin films [103, 104] and dental implants [105]. In addition, the edge extraction and segmentation techniques used in feature characterization have important application prospects in structural surfaces (micro-electromechanical) [106], random surfaces (grinding-wheel morphology), and rapid automatic detection.

Table 6. Some applications for areal feature parameters.

Application \ Symbol	S_{pd}	S_{pc}	S_{10z}	S_{5p}	S_{5v}	$S_{da}(c)$	$S_{ha}(c)$	$S_{dv}(c)$	$S_{hv}(c)$	References
Flat lapping		√	√	√	√	√	√			[100]
Grinding	√	√	√	√					√	
Vertical milling		√			√		√			
Anisotropic stone surface		√	√	√	√	√				
Laser surface treatment		√								
Vapor blasting	√	√	√	√	√					
Turned surface with burnishing		√				√	√	√	√	
Cartilage wear		√		√			√			[101]
Biomedical titanium surface texture		√	√	√						[102]

3.2.3. Comparison between profile motif method and areal feature characterization

Analyzing the surface texture facilitates control of the manufacturing process and part functions. This includes process monitoring and diagnostics, and control of part functions includes functional prediction and diagnostics. The calculation of profile and areal parameters must take into account surface profile points of the sample and the evaluation area. These parameters characterize surface topography properties and are mainly used to monitor the manufacturing process. However, calculation of the feature parameters requires consideration of the points, lines and areas specified on the surface being measured. The parameters characterize the surface features and their interrelationships, and they have diagnostic functions [107].

Areal feature characterization follows the terms of the hills and dales used in the profile motif method. The profile parameter corresponding to the feature parameter S_{pd} is *RPc* in ISO 4287 Amendment 1. The areal parameter S_z is analogous to the profile parameter *Rt*, but this parameter has a strong sensitivity to outliers and is difficult to apply to the robustness evaluation of surface texture height characteristics. Areal feature characterization uses the segmentation method and identifies the important hills and dales on the areal surface by pruning the change tree. Therefore, the height parameters S_{5p}, S_{5v} and S_{10z} established by this method are more robust. For example, the measured values of S_z of cylinder liner surfaces were greater than S_{10z} with the use of 2.5× and 10× objectives in the literature [108].

Roughness and waviness parameters analysis based on engineering practice is not based on complete mathematics, so analytical results may be unstable. In particular, slight changes such as flipping the profile 180° or analyzing the position with a slight difference can cause large differences in the results. However, important hills and dales on the measured areal surface are considered in areal feature characterization. For example, when analyzing the mating surface, the segmentation method can obtain important peaks by correctly using Wolf pruning, so the identified contact points are more robust.

Segmentation techniques and feature parameters in areal feature characterization have been proposed, but the application of this method in industry is still relatively novel. Area feature characterization has great advantages in extracting features of specific texture for the structured surface. However, this is still difficult for the profile motif method and even other areal roughness parameters. The trend of miniaturization of parts and development of structural surfaces will further expand the application range of areal feature characterization in practical industrial production.

3.3. Fractal methods

An engineering surface can be analyzed using fractal methods over a range of scales. The two basic characteristics of fractals are self-similarity and fractal dimension. The fractal dimension D represents the geometric complexity of the fractal surface and is important in fractal analysis.

The Weierstrass-Mandelbrot fractal function, which was modified by Majumdar et al., can be used to express surface height values in profile fractal methods [109]. The fractal dimension can be found by fitting the slope in a double logarithmic coordinate system of the surface profile power spectrum. Alternatively, it can also be found in the direct space, by the box-counting method, which later on came to be the patchwork method.

In areal fractal methods, the volume-scale plot records the volume information obtained by a morphological closing envelope and a morphological opening envelope of the surface using a square horizontal flat structuring element. Uncertainty can be minimized when using this method to calculate the fractal dimension. The relative area analysis method is based on the patchwork method [110]. The fractal dimension of the relative area analysis method is:

$$D = (\log N)/[\log(1/r)], \tag{2}$$

where N is the number of linear or areal units, profile elements are line segments, areal elements are triangular tiles, and$r$ is the linear scaling ratio. The higher the fractal dimension, the more complex the fractal surface. The fractal dimension is greater than or equal to the Euclidean dimension. The fractal dimension of the profile surface is $1 \leq D \leq 2$ and the fractal dimension of the areal surface is $2 \leq D < 3$. The areal fractal method can be used for adhesion, friction, polishing, dental restoration, porous materials, and elastoplastic contact deformation [111–114]. For example, the areal fractal method was used to obtain the relative area of a surface at different roughness levels, and then a relationship was established with the carburizing performance [115].

Fractal shapes are usually generated by iterative algorithms or formulas, so fractal methods are well suited for research in conjunction with computers. The areal fractal method is developed on the basis of the profile fractal method. The range of the fractal is mainly limited by the measurement area and sampling interval. Multi-directional profile fractal analysis can be used to characterize the anisotropy of the surface being measured. The areal fractal method has excellent development prospects in surface design and manufacturing.

4. Conclusions

The connections and distinctions between profile and areal surface roughness from the aspects of characterization and application have been reviewed in this paper.

The areal parameters in principle capture much more of the complexity of surfaces and provide much better understanding of surface morphology than traditional profile parameters, and will be the future direction of development in the field. For example, profile parameters may be limited and misleading when the surface is anisotropic. However, it should be noticed that the profile roughness parameters are still dominant in the factory for surface quality evaluation at present because the current international standards of two-dimensional measurement and characterization are relatively complete. For example, some areal filtering standards are under development, such as spline filters and morphological areal filters. Furthermore, it does not mean that three -dimensional surface measurement and characterization can totally replace the two -dimensional surface measurement and characterization although areal roughness measurement has many advantages over the profile. For example, two dimensional parameters can be easily used

to characterize the turning surface. In the industry, the profile parameter can better characterize the paint on a steel surface. Therefore, profile parameters still have a certain value in the study of longer-wavelength components on the surface or when there is a requirement of the measurement cost control.

In the precision and ultra-precision fields, the surface function of parts is becoming more and more demanding. The measurement and characterization of structured surfaces and freeform surfaces have become a research hotspot. The development of surface roughness presents the following trend: profile standards are being incorporated into areal standard systems, ?ltration techniques and characterization methods are at the forefront of the areal roughness field, the correlations between the surface roughness parameters and the functions need to be further studied, and areal roughness measurement is experiencing intelligent integration of online measurement, high precision and high efficiency.

Acknowledgement

This work is supported by the National Natural Science Foundation of China (51635001).

References

[1] Whitehouse, D. J. (1997). Surface metrology. *Measurement Science and Technology*, *8*(9), 955. https://doi.org/10.1088/0957-0233/8/9/002

[2] Abbott, E. J. & Firestone, F. A. (1933). Specifying Surface Quality. A Method Based on Accurate Measurement and Comparison. *Journal of Mechanical Engineering*, *55*, 569–572.

[3] Schmaltz, G. (1936). *Oberflächenbeschaffenheit und Passungen:* II. Mitteilung PreBsits. Journal of the Japan Society of Precision Engineering, *4*, 268–276.

[4] Leach, R. K. (2014). *Fundamental principles of engineering nanometrology* (2nd ed.). Amsterdam: Elsevier. https://doi.org/10.1016/C2012-0-06010-3

[5] Williamson, J. B. P. (1967). Microtopography of surfaces. *Proceedings of the Institution of Mechanical Engineers, Conference Proceedings*. England, *182*(11), 21-30. https://doi.org/10.1243/PIME_CONF_1967_182_300_02

[6] Nayak, P. R. (1971). Random process model of rough surfaces. *Journal of Lubrication Technology*, *93*(3), 398-407. https://doi.org/10.1115/1.3451608

[7] Sayles, R. S., Thomas, T. R., Anderson, J., Haslock, I., & Unsworth, A. (1979). Measurement of the surface microgeometry of articular cartilage. *Journal of Biomechanics*, *12*(4), 257–267. https://doi.org/10.1016/0021-9290(79)90068-x

[8] De Chiffre, L., & Nielsen, H. S. (1987). A digital system for surface roughness analysis of plane and cylindrical parts. *Precision Engineering*, *9*(2), 59–64. https://doi.org/10.1016/0141-6359(87)90054-7

[9] Thomas, T. R. (2009). Kenneth J. Stout 1941–2006: A memorial. *Wear*, *266*(5–6), 490–497. https://doi.org/10.1016/j.wear.2008.04.053

[10] Mainsah, E., & Stout, K. J. (1993). Second international workshop on the development of methods for the characterization of roughness in 3-D. *Precision Engineering*, *15*(4), 287–288. https://doi.org/10.1016/0141-6359(93)90112-n

[11] E.C. Contract No SMT4-CT98-22561 (1998). The development of a basis for three-dimensional surface roughness standards.

[12] Blateyron F. (2013) The Areal Feature Parameters. In: R. Leach (Eds.), *Characterisation of Areal Surface Texture* (pp. 45–64). Springer. https://doi.org/10.1007/978-3-642-36458-7_3

[13] Blunt, L., & Jiang, X. (2003). *Advanced Techniques for Assessment Surface Topography*. Kogan Page. https://doi.org/10.1016/B978-1-903996-11-9-50015-3

[14] Jiang, X, Scott, P. J., & Whitehouse, D. J. (2003). Paradigm Shifts in Surface Metrology. Part II. The Current Shift. *Proceedings of the Royal Society A. Mathematical Physical & Engineering Sciences*, *463*(2085), 2071–2099. https://doi.org/doi.org/10.1098/rspa.2007.1873 https://

[15] International Organization for Standardization. (2011). *Geometrical Product Specification (GPS) Filtration – Part 21: Linear profile filters: Gaussian filters* (ISO Standard No. 16610-21:2011). https://www.iso.org/standard/50176.html

[16] International Organization for Standardization. (2016). *Geometrical product specifications (GPS) Filtration – Part 31: Robust profile filters: Gaussian regression filters* (ISO Standard No. 16610-31:2016). https://www.iso.org/standard/66242.html

[17] International Organization for Standardization. (2012). *Geometrical Product Specifications (GPS) Surface texture: Areal – Part 3: Specification operators* (ISO Standard No. 25178-3:2012). https://www.iso.org/standard/42895.html

[18] Leach, R. K. (2003). The measurement of surface texture using stylus instruments. *Good Practice Guide No. 37 – National Physical Laboratory*.

[19] Gadelmawla, E. S., Koura, M. M., Maksoud, T. M., Elewa, I. M., & Soliman, H. H. (2002). Roughness parameters. *Journal of Materials Processing Technology*, *123*(1), 133–145. https://doi.org/10.1016/s0924-0136(02)00060-2

[20] Pawlus, P., Reizer, R., & Wieczorowski, M. (2020). Characterization of the shape of height distribution of two-process profile. *Measurement*, *153*, 107387. https://doi.org/10.1016/j.measurement.2019.107387

[21] Yaeger, J. R. D. (2002). Ramp wear and debris from load/unload lift-tab roughness. *IEEE Transactions on Magnetics*, *38*(5), 2126–2128. https://doi.org/10.1109/tmag.2002.802695

[22] Simon, L. B., Khobaib, M., & Matikas, T. E. (1999). Influence of pitting corrosion on structural integrity of aluminum alloys. Nondestructive Evaluation of Aging Materials and Composites III. *International Society for Optics and Photonics*, *3585*, 40-47. https://doi.org/10.1117/12.339861

[23] Fujimura, N., Nakamura, T., Oguma, H. (2013). Application of surface roughness parameters to the evaluation of low cycle fatigue damage in austenitic stainless steel. *ASME 2013 Pressure Vessels and Piping Conference*. American Society of Mechanical Engineers. Digital Collection. https://doi.org/10.1115/pvp2013-97887

[24] Tsukamoto, N. (1984). Investigation about Load Capacity of Nylon Gears, when Tooth Surface Finishing of Mating Steel Gears is different: 2nd Report; Abrasion of Nylon Gear Meshing with Ground Steel Gear. *Bulletin of JSME*, *27*(229), 1529–1536. https://doi.org/10.1299/jsme1958.27.1529

[25] Kopeliovich, D. (2011). Geometry and dimensional tolerances of engine bearings. *Engine professional*, *AERA*, 70–76.

[26] Ochi, M., Gotou, H., Okuno, H., & Taketomi, Y. (2009). Electrode of aluminum-alloy film with low contact resistance, method for production thereof, and display unit (U.S. Patent No. 12/136,409).

[27] Eriksson, R., Sjöström, S., Brodin, H., Johansson, S., Östergren, L., & Li, X. H. (2013). TBC bond coat–top coat interface roughness: Influence on fatigue life and modelling aspects. *Surface and Coatings Technology*, *236*, 230–238. https://doi.org/10.1016/j.surfcoat.2013.09.051

[28] Frost, F., Schindler, A., & Bigl, F. (1998). Ion beam smoothing of indium-containing III-V compound semiconductors. *Applied Physics A*, *66*(6), 663–668. https://doi.org/10.1007/s003390050730

[29] Kumar, S., Batish, A., Singh, R., & Singh, T. P. (2014). A hybrid Taguchi-artificial neural network approach to predict surface roughness during electric discharge machining of titanium alloys. *Journal of Mechanical Science and Technology*, *28*(7), 2831–2844. https://doi.org/10.1007/s12206-014-0637-x

[30] Stout, K. J., & Spedding, T. A. (1982). The characterization of internal combustion engine bores. *Wear*, *83*(2), 311-326. https://doi.org/10.1016/0043-1648(82)90186-7

[31] Lochynski, P., Kowalski, M., Szczygiel, B., & Kuczewski, K. (2016). Improvement of the stainless -steel electropolishing process by organic additives. *Polish Journal of Chemical Technology*, *18*(4), 76–81. https://doi.org/10.1515/pjct-2016-0074

[32] Boscher, N. D., Vaché, V., Carminati, P., Grysan, P., & Choquet, P. (2014). A simple and scalable approach towards the preparation of superhydrophobic surfaces – importance of the surface roughness skewness. *Journal of Materials Chemistry A*, *2*(16), 5744–5750. https://doi.org/10.1039/c4ta00366g

[33] García-Jurado, D., Vazquez-Martinez, J. M., Gámez, A. J., Batista, M., Puerta, F. J., & Marcos, M. (2015). FVM based study of the Influence of Secondary Adhesion Tool Wear on Surface Roughness of Dry Turned Al-Cu Aerospace Alloy. *Procedia Engineering*, *132*, 600–607. https://doi.org/10.1016/j.proeng.2015.12.537

[34] Grzesik, W., & Brol, S. (2009). Wavelet and fractal approach to surface roughness characterization after finish turning of different workpiece materials. *Journal of Materials Processing Technology*, *209*(5), 2522–2531. https://doi.org/10.1016/j.jmatprotec.2008.06.009

[35] Wieland, M., Textor, M., Spencer, N. D., & Brunette, D. M. (2001). Wavelength-dependent roughness: A quantitative approach to characterizing the topography of rough titanium surfaces. *International Journal of Oral & Maxillofacial Implants*, *16*(2).

[36] Wu, J., Dong, J., Wang, Y., & Gond, B. K. (2017). Thermal oxidation ageing effects on silicone rubber sealing performance. *Polymer Degradation and Stability*, *135*, 43–53. https://doi.org/10.1016/j.polymdegradstab.2016.11.017

[37] Matsumoto, R., Kai, N., Tomita, Y., Kajioka, A., Mori, S., & Utsunomiya, H. (2017). Characterization of surface profile of shot peened cemented tungsten carbide dies with micro valleys and their lubrication performance in cold forging. *Procedia Engineering*, 207, 1135–1140. https://doi.org/10.1016/j.proeng.2017.10.1138

[38] Brackbill, T. P., & Kandlikar, S. G. (2006). Effect of triangular roughness elements on pressure drop and laminar-turbulent transition in microchannels and minichannels. *ASME 4th International Conference on Nanochannels, Microchannels, and Minichannels. American Society of Mechanical Engineers Digital Collection*, *47608*, 747–755. https://doi.org/10.1115/icnmm2006-96062

[39] Gualtieri, E., Pugno, N., Rota, A., Spagni, A., Lepore, E., & Valeri, S. (2011). Role of roughness parameters on the tribology of randomly nano-textured silicon surface. *Journal of Nanoscience and Nanotechnology*, *11*(10), 9244–9250. https://doi.org/10.1166/jnn.2011.4296

[40] Cabanettes, F., & Rosén, B. G. (2014). Topography changes observation during running-in of rolling contacts. *Wear*, *315*(1–2), 78–86. https://doi.org/10.1016/j.wear.2014.04.009

[41] Neslusan, M., Hrabovsky, T., & Cillikova, M. (2015). Barkhausen Noise Emission in Milled Surfaces. *Communications-Scientific letters of the University of Zilina*, *17*(3), 57-61.

[42] Yin, Q., Li, C., Dong, L., Bai, X., Zhang, Y., Yang, M., Jia, D., Hou, Y., Liu, Y. & Li, R. (2018). Effects of the physicochemical properties of different nanoparticles on lubrication performance and experimental evaluation in the NMQL milling of Ti–6Al–4V. *The International Journal of Advanced Manufacturing Technology*, *99*(9), 3091–3109. https://doi.org/10.1007/s00170-018-2611-8

[43] International Organization for Standardization. (1996). *Geometrical Product Specification (GPS) – Surface texture: Profile method – Surfaces having stratified functional properties – Part 2: Height characterization using the linear material ratio curve* (ISO Standard No. 13565-2:1996). https://www.iso.org/standard/22280.html

[44] Dimkovski, Z. (2006). *Characterization of a cylinder liner surface by roughness parameters analysis* [Student thesis, Blekinge Institute of Technology]. http://urn.kb.se/resolve?urn=urn:nbn:se:bth-5718 http://urn.kb.se/resolve?urn= urn:nbn:se:bth-5718

[45] Javadi, H., Jomaa, W., Texier, D., Brochu, M., & Bocher, P. (2017). Surface Roughness Effects on the Fatigue Behavior of As-Machined Inconel718. *Solid State Phenomena*, *258*, 306–309. https://doi.org/10.4028/www.scientific.net/ssp.258.306

[46] Pawlus, P., Cieslak, T., & Mathia, T. (2009). The study of cylinder liner plateau honing process. *Journal of Materials Processing Technology*, *209*(20), 6078–6086. https://doi.org/10.1016/j.jmatprotec.2009.04.025

[47] Whitehouse, D. J. (1994). Handbook of Surface Metrology. CRC Press. https://doi.org/10.1016/0141-6359(94)90233-X

[48] Whitehouse, D. J., & Phillips, M. J. (1982). Two-dimensional properties of random surfaces. *Philosophical Transactions of the Royal Society of London. Series A, Mathematical and Physical Sciences*, *305*(1490), 441–468. https://doi.org/10.1098/rsta.1982.0043

[49] Lonardo, P. M., Trumpold, H., & De Chiffre, L. (1996). Progress in 3D surface microtopography characterization. *CIRP Annals*, *45*(2), 589–598. https://doi.org/10.1016/s0007-8506(07)60513-7

[50] Blateyron, F. (2013). The Areal Field Parameters. In: R. Leach (Eds.), *Characterisation of Areal Surface Texture* (pp. 15–43). Springer. https://doi.org/10.1007/978-3-642-36458-7_2

[51] Filipova, N., & Rudzitis, J. (2013). Surface Texture Parameters Application for Nanocoatings. *Transport and Engineering. Production Technologies*, *35*, 118–124.

[52] Annunziata, M., Oliva, A., Basile, M. A., Giordano, M., Mazzola, N., Rizzo, A., Lanza, A., & Guida, L. (2011). The effects of titanium nitride-coating on the topographic and biological features of TPS implant surfaces. *Journal of Dentistry*, *39*(11), 720–728. https://doi.org/10.1016/j.jdent.2011.08.003

[53] Sedlaček, M., Gregorčič, P., & Podgornik, B. (2017). Use of the roughness parameters S sk and S ku to control friction – A method for designing surface texturing. *Tribology Transactions*, *60*(2), 260–266. https://doi.org/10.1080/10402004.2016.1159358

[54] Ereifej, N. S., Oweis, Y. G., & Eliades, G. (2012). The effect of polishing technique on 3-D surface roughness and gloss of dental restorative resin composites. *Operative Dentistry*, *38*(1), E9–E20. https://doi.org/10.2341/12-122-l

[55] Löberg, J., Mattisson, I., Hansson, S., & Ahlberg, E. (2010). Characterisation of titanium dental implants I: critical assessment of surface roughness parameters. *The Open Biomaterials Journal*, *2*(1), 18-35. https://doi.org/10.2174/1876502501002010018

[56] Berglund, J., Brown, C. A., Rosen, B. G., & Bay, N. (2010). Milled die steel surface roughness correlation with steel sheet friction. *CIRP Annals*, *59*(1), 577–580. https://doi.org/10.1016/j.cirp.2010.03.140

[57] Kalisz, J., Zak, K., Grzesik, W., & Czechowski, K. (2015). Characteristics of Surface Topography after Rolling Burnishing of EM AW-AlCu4MgSi (A) Aluminium Alloy. *Journal of Machine Engineering*, *15*(1), 71–80.

[58] Waterworth, A. (2006). *Quantitative characterisation of surface finishes on stainless steel sheet using 3D surface topography analysis* [Doctoral dissertation, University of Huddersfield]. https://ethos.bl.uk/OrderDetails.do?uin=uk.bl.ethos.445085

[59] Rubach, S., Riemer, T., Valentin, J., & Delto, C. (2014). Wear detection on cylinder liners with optical 3D measuring technology. *MTZ worldwide*, *75*(3), 38–43. https://doi.org/10.1007/s38313-014-0032-0

[60] Zhong, Z. W., Lu, Y. G. (2002). 3D characterization of super-smooth surfaces of diamond turned OFHC copper mirrors. *Materials and Manufacturing Processes*, *17*(3), 387–399. https://doi.org/10.1081/amp-120005384

[61] Cresti, S., Itri, A., Rebaudi, A., Diaspro, A., & Salerno, M. (2015). Microstructure of Titanium-Cement-Lithium Disilicate Interface in CAD-CAM Dental Implant Crowns: A Three-Dimensional Profilometric Analysis. *Clinical Implant Dentistry & Related Research*, *17*, 97–106. https://doi.org/10.1111/cid.12133

[62] Derchi, G., Vano, M., Barone, A., Covani, U., Diaspro, A., & Salerno, M. (2017). Bacterial adhesion on direct and indirect dental restorative composite resins: An invitro study on a natural biofilm. *Journal of Prosthetic Dentistry*, *117*(5), 669–676. https://doi.org/10.1016/j.prosdent.2016.08.022

[63] Salerno, M., Caneva-Soumetz, F., Pastorino, L., Patra, N., Diaspro, A., & Ruggiero, C. (2013). Adhesion and proliferation of osteoblast-like cells on anodic porous alumina substrates with different morphology. *IEEE Transactions on Nanobioscience*, *12*(2), 106–111. https://doi.org/10.1109/tnb.2013.2257835

[64] Salerno, M., Loria, P., Matarazzo, G., Tomè, F., Diaspro, A., & Eggenhöffner, R. (2016). Surface morphology and tooth adhesion of a novel nanostructured dental restorative composite. *Materials*, *9*(3). https://doi.org/10.3390/ma9030203

[65] Bulaha, N., & Rudzitis, J. (2018). Calculation possibilities of 3D parameters for surfaces with irregular roughness. *Latvian Journal of Physics and Technical Sciences*, *55*(4), 70–79. https://doi.org/10.2478/lpts-2018-0030

[66] Madej, M., Kowalczyk, J., Ozimina, D., & Milewski, K. (2018). The Tribological Properties of Titanium Carbonitride TiCN Coating Lubricated with Non-Toxic Cutting Fluid. *Materials Research Proceedings*, *5*, 47–53. https://doi.org/10.21741/9781945291814-9

[67] Sedlaček, M., Podgornik, B., & Vižintin, J. (2012). Correlation between standard roughness parameters skewness and kurtosis and tribological behaviour of contact surfaces. *Tribology International*, *48*, 102–112. https://doi.org/10.1016/j.triboint.2011.11.008

[68] Ţălu, Ş., Patra, N., & Salerno, M. (2015). Micromorphological characterization of polymer-oxide nanocomposite thin films by atomic force microscopy and fractal geometry analysis. *Progress in Organic Coatings*, *89*, 50–56. https://doi.org/10.1016/j.porgcoat.2015.07.024

[69] Salerno, M., Reverberi, A. P., & Baino, F. (2018). Nanoscale topographical characterization of orbital implant materials. *Materials*, *11*(5), 660. https://doi.org/10.3390/ma11050660

[70] Prajapati, D. K., & Tiwari, M. (2019). Assessment of topography parameters during running-in and subsequent rolling contact fatigue tests. *Journal of Tribology*, *141*(5). https://doi.org/10.1115/1.4042676

[71] Schulz, E., Calandra, I., Kaiser, T. M. (2010). Applying tribology to teeth of hoofed mammals. *Scanning*, *32*(4), 162–182. https://doi.org/10.1002/sca.20181

[72] Li, Q., Yang, G., Wang, K. C., Zhan, Y., & Wang, C. (2017). Novel macro-and microtexture indicators for pavement friction by using high-resolution three-dimensional surface data. *Transportation Research Record*, *2641*(1), 164–176. https://doi.org/10.3141/2641-19

[73] Reizer, R., Pawlus, P. (2011). 3D surface topography of cylinder liner forecasting during plateau honing process. *In Journal of Physics: Conference Series*. IOP Publishing, *311*(1), 012021. https://doi.org/10.1088/1742-6596/311/1/012021

[74] Jiang, X. Q., & Blunt, L. (2003). Surface analysis techniques to optimise the performance of CNC machine tools. *WIT Transactions on Engineering Sciences*, *44*.

[75] Biondani, F. G., Bissacco, G., Pilný, L. & Hansen, H. N. (2019). Analysis and Characterization of Machined Surfaces with Aesthetic Functionality. *International Journal of Automation Technology*, *13*(2), 261–269. https://doi.org/10.20965/ijat.2019.p0261

[76] Islamova, A., & Ponomarev, K. (2019). Wetting and spreading of droplets on rough aluminum surfaces. *In EPJ Web of Conferences*. EDP Sciences, *196*, 00024. https://doi.org/10.1051/epjconf/201919600024

[77] Sul, Y. T., Kang, B. S., Johansson, C., Um, H. S., Park, C. J., & Albrektsson, T. (2009). The roles of surface chemistry and topography in the strength and rate of osseointegration of titanium implants in bone. *Journal of Biomedical Materials Research Part A*, *89*(4), 942–950. https://doi.org/10.1002/jbm.a.32041

[78] Salerno, M., Itri, A., Frezzato, M., & Rebaudi, A. (2015). Surface Microstructure of Dental Implants Before and After Insertion: An In Vitro Study by Means of Scanning Probe Microscopy. *Implant Dentistry*, *24*(3), 248–255.

[79] Stoica, I., Barzic, A. I., & Hulubei, C. (2013). The impact of rubbing fabric type on surface roughness and tribological properties of some semi-alicyclic polyimides evaluated from atomic force measurements. *Applied Surface Science*, *268*, 442–449. https://doi.org/10.1016/j.apsusc.2012.12.123

[80] Dzierwa, A., Reizer, R., Pawlus, P., & Grabon, W. (2014). Variability of areal surface topography parameters due to the change in surface orientation to measurement direction. *Scanning: The Journal of Scanning Microscopies*, *36*(1), 170–183. https://doi.org/10.1002/sca.21115

[81] Wizner, M., Jakubiec, W., & Starczak, M. (2011). Description of surface topography of sealing rings. *Wear*, *271*(3-4), 571–575. https://doi.org/10.1016/j.wear.2010.04.036

[82] Waikar, R. A., & Guo, Y. B. (2008). A comprehensive characterization of 3D surface topography induced by hard turning versus grinding. *Journal of Materials Processing Technology*, *197*(1–3), 189–199. https://doi.org/10.1016/j.jmatprotec.2007.05.054

[83] Alipour, R., Riazifar, M. R., & Afsari, T. (2016). The effect of pressure on morphological features and quality of synthesized graphene. *Research on Chemical Intermediates*, *42*(12), 8261–8272. https://doi.org/10.1007/s11164-016-2594-8

[84] Casoli, A., Cremonesi, P., Isca, C., Groppetti, R., Pini, S., & Senin, N. (2013). Evaluation of the effect of cleaning on the morphological properties of ancient paper surface. *Cellulose*, *20*(4), 2027–2043. https://doi.org/10.1007/s10570-013-9975-6

[85] Ţălu, Ş., Bramowicz, M., Kulesza, S., Pignatelli, F., & Salerno, M. (2017). Surface Morphology Analysis of Composite Thin Films based on Titanium-Dioxide Nanoparticles. *Acta Physica Polonica, A.*, *131*(6), 1529–1533. https://doi.org/10.12693/aphyspola.131.1529

[86] Qi, Q., Liu, X., & Jiang, X. (2009). Functions and three -dimensional parameters of surface texture. *In Fifth International Symposium on Instrumentation Science and Technology*. International Society for Optics and Photonics, *7133*, 713303. https://doi.org/10.1117/12.811358

[87] Clare, A. T., Speidel, A., Mitchell-Smith, J., & Patwardhan, S. (2017). Electrolyte design for suspended particulates in electrolyte jet processing. *CIRP Annals*, *66*(1), 201–204. https://doi.org/10.1016/j.cirp.2017.04.133

[88] Mironov, V., Stankevich, P., Tatarinov, A., Zemchenkov, V., & Boiko, I. (2015, October). Mechanical and Acoustical Properties of Bushings Made of Low-Alloyed Materials and Used in Brake Systems of Transport Vehicles. *In IOP Conference Series: Materials Science and Engineering*. IOP Publishing, *6*(1), 0120169. https://doi.org/10.1088/1757-899x/96/1/012016

[89] Baglin, K. P. (1986). Micro-elastohydrodynamic lubrication and its relationship with running-in. *Proceedings of the Institution of Mechanical Engineers, Part C: Journal of Mechanical Engineering Science*, *200*(6), 415–424. https://doi.org/10.1243/pime_proc_1986_200_150_02

[90] Ohlsson, R., Rosén, B. G., & Westberg, J. (2003). The interrelationship of 3D surface characterisation techniques with standardised 2D techniques. In L. Blunt, X. Jiang (Eds.), *Advanced Techniques for Assessment Surface Topography: Development of a Basis for 3D Surface Texture Standards "SURFSTAND"* (pp. 197–220). Kogan Page Science. https://doi.org/10.1016/b978-190399611-9/50008-6

[91] Grzesik, W., Rech, J., & Żak, K. (2015). Characterization of surface textures generated on hardened steel parts in high-precision machining operations. *The International Journal of Advanced Manufacturing Technology*, *78*(9–12), 2049–2056. https://doi.org/10.1007/s00170-015-6800-4

[92] Deleanu, L., Georgescu, C., & Suciu, C. (2012). A comparison between 2D and 3D surface parameters for evaluating the quality of surfaces. *The Annals of "Dunarea de Jos" University of Galati, Fascicle V, Technologies in Machine Building*, *30*(1), 5–12.

[93] Pawlus, P., Reizer, R., & Wieczorowski, M. (2018). Comparison of results of surface texture measurement obtained with stylus methods and optical methods. *Metrology and Measurement Systems*, *25*(3), 589–602. https://doi.org/10.1515/mms-2017-0046

[94] Bárányi, I., Czifra, Á., & Kalácska, G. (2011). Height-independent topographic parameters of worn surfaces. *Sustainable Construction and Design*, *2*(1), 35.

[95] Blunt, L., & Jiang, X. (2003). Numerical Parameters for Characterisation of Topography. In L. Blunt, X. Jiang (Eds.), *Advanced Techniques for Assessment Surface Topography: Development of a Basis for 3D Surface Texture Standards "SURFSTAND"* (pp. 17–41). Kogan Page Science. https://doi.org/10.1016/b978-190399611-9/50002-5

[96] Pawlus, P., Reizer, R., Wieczorowski, M., & Krolczyk, G. (2020). Material ratio curve as information on the state of surface topography – A review. *Precision Engineering*, *65*, 240–258. https://doi.org/10.1016/j.precisioneng.2020.05.008

[97] Jiang, X. Q., Blunt, L., Stout, K. J. (2010). Comparison study of areal functional parameters for rough surfaces. Proc ASPE, Nashville.

[98] Fahl, C. F. (1982). Motif combination—a new approach to surface profile analysis. *Wear*, *83*(1), 165–179. https://doi.org/10.1016/0043-1648(82)90349-0

[99] International Organization for Standardization. (1996). *Geometrical Product Specification (GPS) – Surface texture: Profile method – Motif parameters* (ISO Standard No. 12085:1996). https://www.iso.org/standard/20867.html

[100] Pawlus, P., Graboń, W., & Reizer, R. (2013). Variation of areal parameters on machined surfaces. *11th International Symposium on Measurement and Quality Control*, Poland.

[101] Tian, Y., Wang, J., Peng, Z., & Jiang, X. (2011). Numerical analysis of cartilage surfaces for osteoarthritis diagnosis using field and feature parameters. *Wear*, *271*(9–10), 2370–2378. https://doi.org/10.1016/j.wear.2011.01.081

[102] Wang, J., Jiang, X., Gurdak, E., Scott, P., Leach, R., Tomlins, P., & Blunt, L. (2011). Numerical characterisation of biomedical titanium surface texture using novel feature parameters. *Wear*, *271*(7–8), 1059–1065. https://doi.org/10.1016/j.wear.2011.05.018

[103] Stach, S., Dallaeva, D., Ţalu, Ş., Kaspar, P., Tománek, P., Giovanzana, S., & Grmela, L. (2015). Morphological features in aluminum nitride epilayers prepared by magnetron sputtering. *Materials Science-Poland*, *33*(1), 175–184. https://doi.org/10.1515/msp-2015-0036

[104] Ţălu, Ş., Ghazai, A. J., Stach, S., Hassan, A., Hassan, Z., & Ţălu, M. (2014). Characterization of surface roughness of Pt Schottky contacts on quaternary n-Al 0.08 In 0.08 Ga 0.84 N thin film assessed by atomic force microscopy and fractal analysis. *Journal of Materials Science: Materials in Electronics*, *25*(1), 466–477. https://doi.org/10.1007/s10854-013-1611-6

[105] Glon, F, Flys, O., & Lööf, P. J. (2014). 3D SEM for surface topography quantification – a case study on dental surfaces. In *Journal of Physics: Conference Series*. IOP Publishing, *483*(1), *012026*. https://doi.org/10.1088/1742-6596/483/1/012026

[106] Blanc, J., Grime, D., & Blateyron, F. (2011). Surface characterization based upon significant topographic features. In *Journal of Physics: Conference Series*. IOP Publishing, *311*(1), 012014. https://doi.org/10.1088/1742-6596/311/1/012014

[107] Scott, P. J. (2009). Feature parameters. *Wear*, *266*(5-6), 548–551. https://doi.org/10.1016/j.wear.2008.04.056

[108] Dimkovski, Z., Ohlsson, R., & Rosén, B. G. (2014). Effect of the measurement size on the robustness of the assessment of the features specific for cylinder liner surfaces. *Surface Topography: Metrology and Properties*, *2*(1), 014013. https://doi.org/10.1088/2051-672x/2/1/014013

[109] Majumdar, A., & Tien, C. L. (1990). Fractal characterization and simulation of rough surfaces. *Wear*, *136*(2), 313–327. https://doi.org/10.1016/0043-1648(90)90154-3

[110] Brown, C. A., Charles, P. D., Johnsen, W. A., & Chesters, S. (1993). Fractal analysis of topographic data by the patchwork method. *Wear*, *161*(1–2), 61–67. https://doi.org/10.1016/0043-1648(93)90453-s

[111] Brown, C. A., & Siegmann, S. (2001). Fundamental scales of adhesion and area–scale fractal analysis. *International Journal of Machine Tools and Manufacture*, *41*(13–14), 1927–1933. https://doi.org/10.1016/s0890-6955(01)00057-8

[112] Salerno, M., Giacomelli, L., & Derchi, G. (2010). Atomic force microscopy in vitro study of surface roughness and fractal character of a dental restoration composite after air-polishing. *Biomedical Engineering online*, *9*(1), 59. https://doi.org/10.1186/1475-925x-9-59

[113] Jian-Chao, C., Bo-Ming, Y., & Ming-Qing, Z. (2010). Fractal analysis of surface roughness of particles in porous media. *Chinese Physics Letters*, *27*(2), 024705. https://doi.org/10.1088/0256-307x/27/2/024705

[114] Goedecke, A., Jackson, R. L., Mock, R. (2013). A fractal expansion of a three -dimensional elastic-plastic multi-scale rough surface contact model. *Tribology International*, *59*, 230–239. https://doi.org/10.1016/j.triboint.2012.02.004

[115] Karabelchtchikova, O., Brown, C. A., & Sisson, R. D. (2007). Effect of surface roughness on kinetics of mass transfer during gas carburising. *International Heat Treatment and Surface Engineering*, *1*(4), 164–170. https://doi.org/10.1179/174951507x264991

Baofeng He received both her B.Sc. degree and M.Sc. degrees from Harbin Institute of Technology in 2006 and 2009 respectively, and the Ph.D. degree from Loughborough University in UK in 2012. Currently, she is a lecturer at Beijing University of Technology. Her main research interests are precision measurement technology and instruments.

Siyuan Ding received his B.Eng. degree from Zhengzhou University in 2016 and M.Eng. degree from Beijing University of Technology in 2020. His main research interests are precision measurement technology and instruments.

Zhaoyao Shi received his B.Sc. degree from Hefei University of Technology in 1984 and the M.Sc. degree from Shanxi Institute of Mechanical Engineering in 1988, and the Ph.D. degree from Hefei University of Technology in 2001. Currently, he is Professor and a Ph.D. supervisor at Beijing University of Technology, and a "Yangtze River Scholar" special professor awarded by the Ministry of Education. His main research interests are precision measurement technology and instruments.